



# Sensorineural Hearing Loss Through the Ages

David T. Wang, MBBS,<sup>\*,†</sup>, Raghu Ramakrishnaiah, MBBS,<sup>‡</sup> and Alisa Kanfi, MD<sup>\*,†</sup>

## Introduction

Hearing loss is a common symptom both in children and adults and is typically categorized as conductive, sensorineural, or mixed. In children, 1-2 in 1000 are diagnosed with sensorineural hearing loss.<sup>1</sup> The overall prevalence of hearing impairment in the adult population is 14%, which disproportionately affects the older age group with up to 43% of those aged 65-84 years affected.<sup>2</sup> Sensorineural hearing loss etiologies can be either cochlear in location or retrocochlear, meaning beyond the inner ear involving the 8th cranial nerve or other portions of the brain involved with auditory processing. Infection and traumatic causes of sensorineural hearing loss occur in both adult and pediatric populations. A common etiology of sensorineural hearing loss in children is congenital malformations. In adults, the most common cause is presbycusis, which unfortunately for the radiologist, occurs at the microscopic level and is beyond the resolution of computed tomography (CT) and magnetic resonance imaging (MRI). Common causes of adult sensorineural hearing loss appreciable on imaging include otosclerosis and retrocochlear masses.

## Anatomy

While temporal bone anatomy has plagued radiology trainees throughout time, a simple understanding of the anatomy and function of the middle and inner ear structures enables the radiologist to make accurate and clinically relevant diagnoses. Sensorineural hearing loss may be the result of an abnormality in the inner ear structures (cochlea, vestibule, and semicircular canals), the internal auditory canal (IAC)

containing the seventh and eighth cranial nerves, or the bony labyrinth (otic capsule) (Fig. 1).

The cochlea is a spiral structure within the temporal bone with  $2\frac{1}{2}$  to  $2\frac{3}{4}$  turns, filled with perilymphatic and endolymphatic fluid. Its purpose is to conduct vibrations from the middle ear ossicles via the oval window at the base of the cochlea to the vibration-sensitive organ of Corti housed within the cochlea. Movement of the hair cells within the organ of Corti is converted into electrical impulses and then relayed via the cochlear nerve to the brainstem. Each cochlear turn is separated by the interscalar septum radiating from the modiolus, the central osseous portion of the cochlea. The round window at the base of the cochlea allows this movement of fluid within the cochlea. The vestibular aqueduct is the osseous canal within the petrous temporal bone containing the endolymphatic sac, which is connected by the endolymphatic duct to the sacculle within the vestibule.

Facial and vestibulocochlear nerves extend from their nuclei within the brainstem through the subarachnoid space to the IAC. Within the IAC, the nerves are separated by a horizontal bone, known as the falciform crest, and a vertical bone at its superior aspect, Bill's bar. Within the IAC, the facial nerve is within the anterior superior quadrant, the cochlear nerve at the anterior inferior quadrant, and the superior and inferior divisions of the vestibular nerve are situated posteriorly (Fig. 2).

## Embryology

Genetic or in-utero insults can result in abnormalities of the inner ear structures, leading to congenital sensorineural hearing loss. The spectrum of cochlear anomalies is linked to the gestational age in which insult occurs so an understanding of the embryologic origin of these inner ear structures can aid in the radiologic interpretation. Development of inner ear starts at 2.5 weeks and is complete by about 26 weeks of gestation. The labyrinth forms from otic placodes, which then invaginate to form the otic vesicle. The cochlear and semicircular canals are ultimately formed from the otic vesicle. The middle ear ossicles are formed from the first and second pharyngeal arches. There is an association

\*Department of Radiology, University of Cincinnati Medical Center, Cincinnati, OH.

†Department of Neuroradiology, University of Cincinnati Medical Center, Cincinnati, OH.

‡University of Arkansas for Medical Sciences, Arkansas Children's Hospital, Little Rock, AR.

Conflict of interest: DTW: None to disclose. RR: None to disclose. AK: None to disclose.

Address reprint requests to Alisa Kanfi, MD, Department of Radiology, University of Cincinnati Medical Center, 234 Goodman Street, ML0761, Cincinnati, OH 45219. E-mail: [kanfiaa@ucmail.uc.edu](mailto:kanfiaa@ucmail.uc.edu)

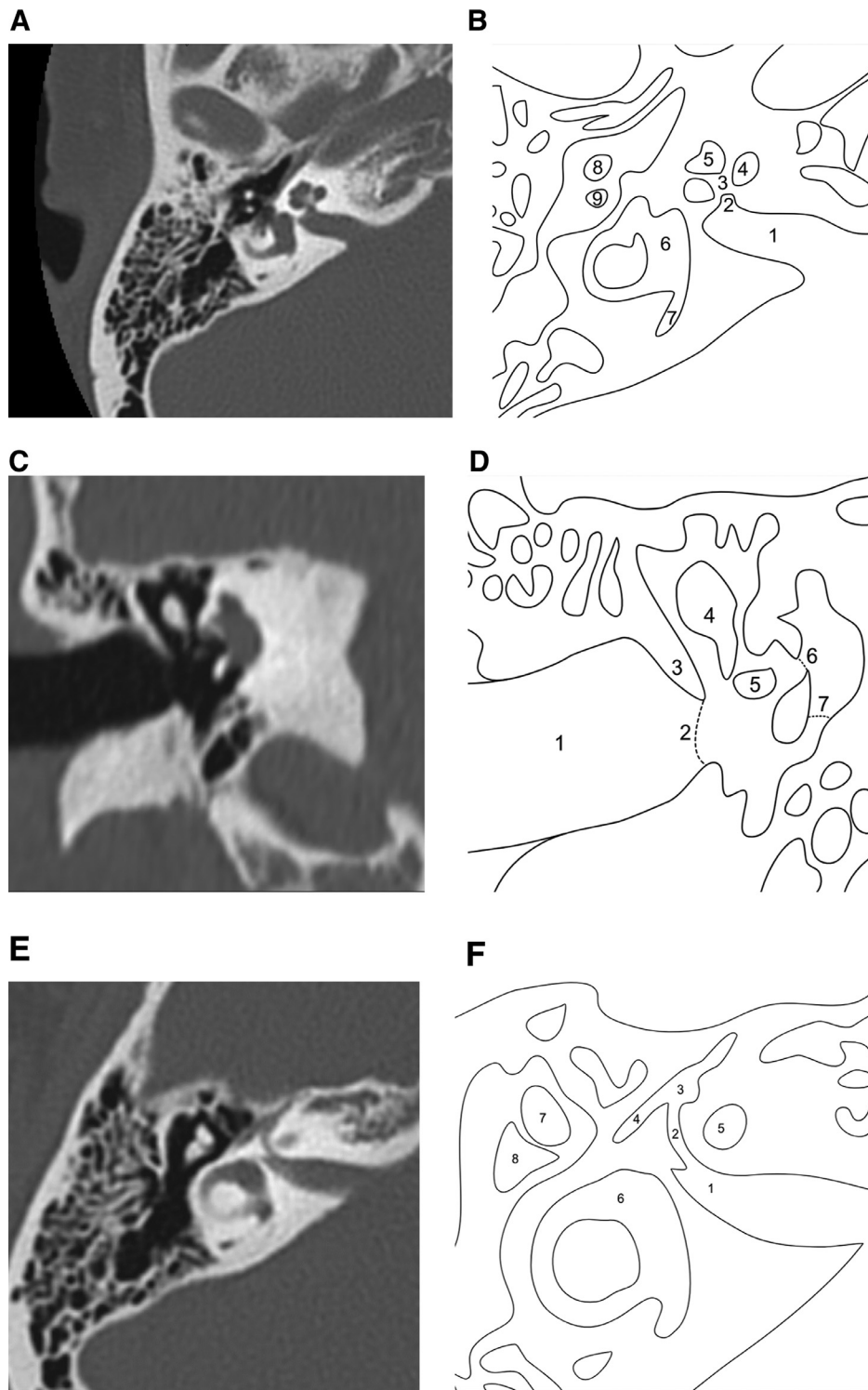


**Figure 1** (A) Axial CT image through the internal auditory canal, demonstrating the cochlear aperture. (B) Line drawing depicting the CT findings. 1 IAC, 2 cochlear aperture, 3 modiolus, 4 basal turn of cochlea, 5 apical turn of cochlea, 6 vestibule, 7 vestibular aqueduct, 8 malleus, 9 incus. (C) Coronal CT image through the external auditory canal, demonstrating the middle ear cavity, oval and round windows. (D) Line drawing depicting the CT findings. 1 external auditory canal, 2 tympanic membrane, 3 scutum, 4 incus, 5 stapes, 6 oval window, 7 round window. (E) Axial CT image through the lateral semicircular canal, demonstrating the labyrinthine and tympanic segments of the facial nerve. (F) Line drawing depicting the CT findings. 1 IAC, 2 labyrinthine segment of the facial nerve, 3 geniculate ganglion, 4 tympanic segment of the facial nerve, 5 partial voluming of cochlea, 6 lateral semicircular canal, 7 malleous, 8 incus.

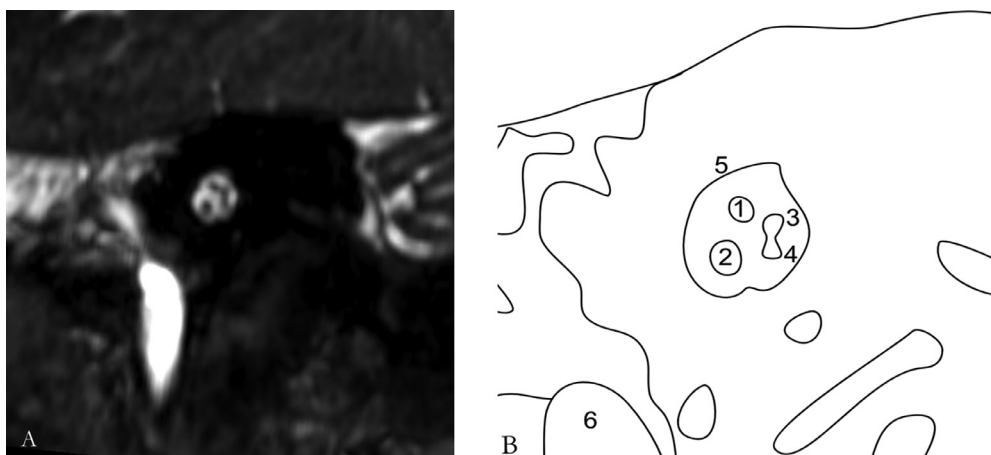


**Figure 2** (A) Sagittal MRI through the internal auditory canal, demonstrating the orientation of the facial and vestibulocochlear nerves. (B) Line drawing depicting the findings on MRI. 1 facial nerve, 2 cochlear nerve, 3 vestibular nerve superior division, 4 vestibular nerve inferior division, 5 IAC, 6 Internal carotid artery.

between inner ear dysplasia and middle or external ear anomalies in 15%-20% of cases.<sup>3</sup>

## Congenital Causes of Sensorineural Hearing Loss

### Enlarged Vestibular Aqueduct

Enlarged vestibular aqueduct is the most common congenital lesion causing sensorineural hearing loss encountered on imaging. Only 32% of children with sensorineural hearing loss have imaging findings and an enlarged vestibular aqueduct is the most common finding.<sup>4</sup> Patients usually present with progressive hearing loss, as well as vertigo and tinnitus. The condition can also be associated with cochlear abnormalities in 84% of cases.<sup>5</sup> While there are varying measurements of the vestibular aqueduct, a measurement larger than 2 mm at the aperture and 1-1.5 mm at the midpoint is considered abnormal.<sup>4</sup> The posterior limb of the posterior semicircular canal is often used as a quick internal control for assessment of enlargement of the endolymphatic sac, housed within the vestibular aqueduct, as the sac should not be larger than the adjacent limb. Approximately 50%-66% of cases are bilateral and close inspection of both vestibular aqueducts is warranted.<sup>6</sup> Enlargement of the endolymphatic duct can be seen directly on high-resolution T2-weighted images on MRI (Fig. 3). Attention to the cochlear partitioning on both the high-resolution T2-weighted imaging and thin-section CT imaging is necessary due to the high association with the enlarged vestibular aqueduct.

### Cochlear Malformations

Cochlear anomalies are seen in 4% of pediatric patients with sensorineural hearing loss.<sup>1</sup> The severity of the cochlear abnormality or deformity depends on the gestational age of insult; the earlier the insult, the more severe and extensive the malformation.

Labyrinthine aplasia is rare and the most severe abnormality due to an insult at the 3rd week of gestation.<sup>7</sup> CT and MRI findings will show complete absence of the cochlea, vestibule, and semicircular canals.

Cochlear aplasia, or complete absence of the cochlea, occurs from an early insult at the late 3rd week of gestation, with the vestibule and semicircular canal still present, but with varying degrees of dysplasia.<sup>8</sup> On CT, there is dense bone in the expected position of the cochlea (Fig. 4). Cochlear aplasia is also rare and only represents 3% of cochlear malformations.<sup>9</sup>

Common cavity malformation presents as the absence of differentiation between the cochlea and vestibule, with a globular cystic structure. This occurs due to insult at the 4th week of gestation.<sup>8</sup> There may be rudimentary semicircular canals present and the middle ear cavity is often normal. This is differentiated from cochlear aplasia by the location of the IAC relative to the cavity. In cochlear aplasia, the vestibule and semicircular canals are in its normal expected position at the posterolateral aspect of the IAC fundus, whereas

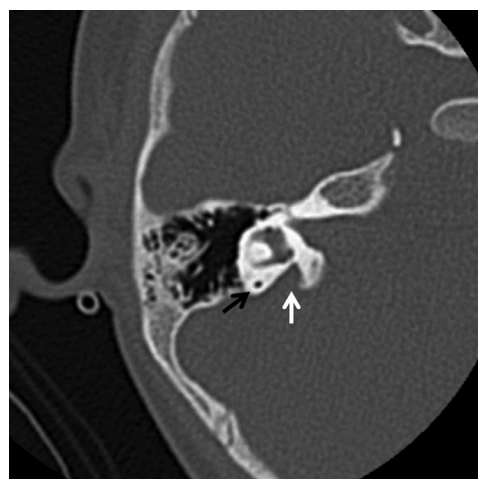


**Figure 3** Axial CT image shows the right vestibular aqueduct is enlarged (white arrow), both by measurement (>2mm) and by the internal control of the posterior limb of the semicircular canal (black arrow). The cochlea was normally partitioned (not pictured).

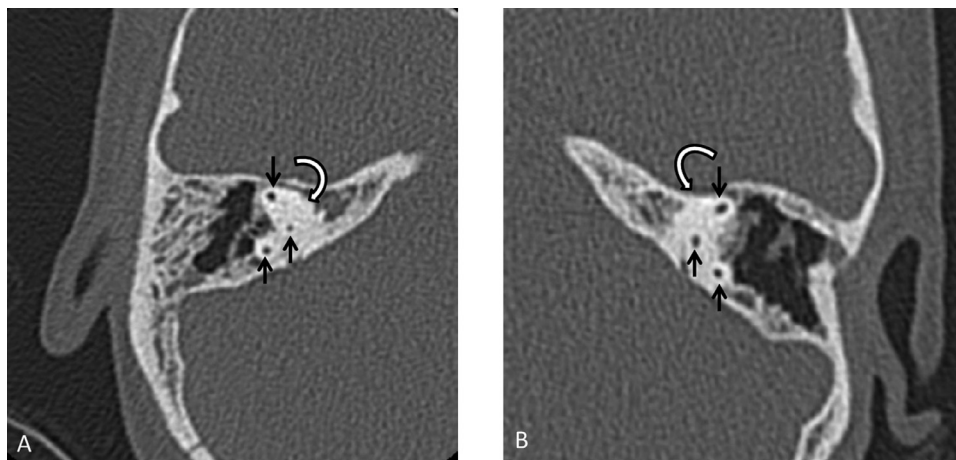


**Figure 4** Axial CT section of the right and left temporal bones (A, B) through the superior and posterior semicircular canals (arrows). Notice absence of the cochlea on both sides (curved arrows).

in common cavity malformations, the IAC fundus is central to the common cavity.<sup>10</sup>

Cochlear incomplete partition type I (IP I) is also known as a cystic cochleovestibular malformation, with an arrest in development arrest in the 5th week of gestation.<sup>11</sup> Imaging demonstrates absence of the modiolus and interscalar septum, with a demarcation between the featureless cochlear and dilated vestibule.<sup>10</sup> This has typically been described as a “Figure 8” appearance, due to the dilated but dysmorphic cochlea and vestibule (Fig. 5). This anomaly occurs in 17% of inner ear malformations.<sup>11</sup>

A cochlear incomplete partition type II (IP II) insult is thought to be at the 7th week of gestation.<sup>11</sup> On imaging, there is a defect of the apical portion of the modiolus and interscalar septum (resulting in a cochlea with 1.5 turns) and an absent interscalar septum. The dysmorphic middle and apical turns are seated asymmetrically on a normal basal turn, resulting in a “baseball cap” appearance of the malformed cochlea (Fig. 6). There is almost always enlargement of the endolymphatic sac with IP II (previously referred to as a Mondini deformity). IP II occurs in 22% of inner ear malformations.<sup>11</sup>

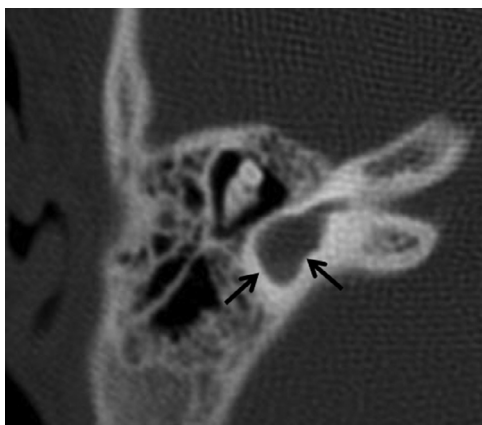


**Figure 5** Axial CT image shows a dilated and dysmorphic cochlea and vestibule of IP1 (arrows), giving a “figure 8” or “snowman” appearance.

### Cochlear Nerve Deficiency and Aperture Abnormality

Cochlear nerve deficiency refers to either an absent or hypoplastic cochlear nerve, which may be unilateral or bilateral. This occurs in 12%-18% of patients with sensorineural hearing loss.<sup>1</sup> The IAC may also be hypoplastic or normal in size. MRI allows visualization of the cochlear nerve within the IAC at the anterior inferior quadrant, particularly on high resolution, volumetric T2-weighted images (Fig. 7).

The cochlear aperture transmits the cochlear nerve from the IAC to the basal turn of the cochlea. A cochlear aperture width of less than 1.4 mm is hypoplastic.<sup>12</sup> An aplastic or hypoplastic cochlear aperture, also called cochlear aperture stenosis, is associated with cochlear nerve hypoplasia and/or aplasia.

### Acquired Causes of Sensorineural Hearing Loss

#### Labyrinthitis Ossificans

Viral or bacterial infection at any age can result in sensorineural hearing loss. Acquired infections can spread from the inner ear meninges or hematogenously. Patients can present with sudden hearing loss, vertigo or tinnitus. In the initial phases of the infection, the CT scan is normal. MRI can demonstrate enhancement of the cochlea, vestibule, or semicircular canals and decreased signal of the endolymph on T2-weighted images. Chronically, the cochlea becomes fibrosed and ossified, known as labyrinthitis ossificans. Eventually, there is complete obliteration and sclerosis of the labyrinth on both CT and MRI (Fig. 8).

#### Trauma

Fractures through the petrous temporal bone can result in sensorineural hearing loss in both adult and pediatric populations. Traditional classification of temporal bone fractures characterized fractures as either longitudinal, transverse or

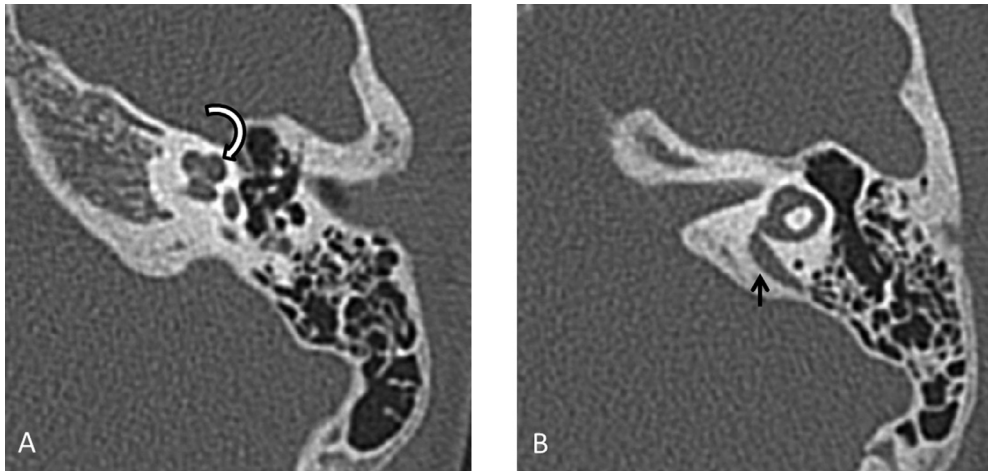


**Figure 6** Axial CT section through the cochlea (A) showing absent modiolus and dysplasia of the apical turn of the cochlea (curved arrow). Axial CT section through the vestibule and semicircular canal (B) showing enlarged vestibular aqueduct (arrow).

mixed. A newer classification emphasizes whether fractures are otic capsule violating or sparing, increasing the prognostic value of the description. Patients with fractures involving the otic capsule are more likely to have sensorineural hearing loss, facial nerve injury and cerebrospinal fluid leak.<sup>13,14</sup> Pneumolabyrinth findings on CT are indicative of disruption of the otic capsule, even if the fracture line is not well-delimited (Fig. 9).

## Otosclerosis

Otosclerosis is an idiopathic progressive process that demineralizes the perilymphatic bone and replaces it with vascular spongiotic bone, resulting in sensorineural, conductive or mixed hearing loss. Typical age of presentation is 20-40 and the process is bilateral in the majority of cases (80%-85%).<sup>15</sup> Otosclerosis can be categorized as fenestral (85% of cases) involving the oval window and stapes footplate, and retrofenestral, involving the cochlea.<sup>6</sup> Early in the disease process,

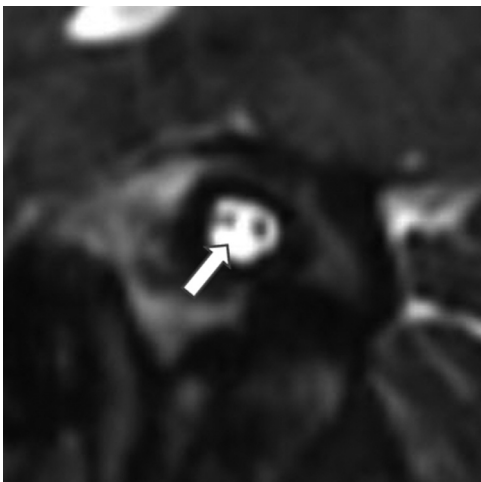


**Figure 7** Oblique MR image through the IAC demonstrates the absence of the cochlear nerve (arrow).

the region anteromedial to the oval window is involved, which can then progress and narrow the oval window and cause fixation of the stapes. Other areas that may be affected include the cochlear promontory, facial nerve canal, and round window. CT demonstrates lucency of the perilymphatic bone in the areas described above (Fig. 10). Eventually, sclerosis may occur. As the temporal bone is one of the densest bones in the human body, any lucency in the bony matrix should be considered abnormal. MRI can show enhancement or increased T2 signal in the affected regions.

## Masses

Brainstem and cerebellopontine angle masses can be a cause of retrocochlear sensorineural hearing loss. A wide spectrum of masses can occur, including schwannomas, meningiomas, lipomas, vascular malformations, metastases, epidermoid, and arachnoid cysts.

Vestibular schwannomas comprise of 70%-80% of extra-axial cerebellopontine angle masses and can extend into and widen the IAC.<sup>16</sup> Bilateral vestibular schwannomas in younger patients should raise the possibility of neurofibromatosis type 2.<sup>17</sup> Otherwise, vestibular schwannomas present at a median age of 50 and are unilateral in greater than 90% of patients.<sup>16</sup> Vestibular schwannomas can protrude out of the IAC, resulting in an “ice cream cone” appearance (Fig. 11). Vestibular schwannomas can also extend along the course of the 8 cranial nerve to involve the cochlea. The lesions are best evaluated on MRI and demonstrate variable T2 signal and avid enhancement.<sup>17</sup>

Meningiomas can typically be differentiated from vestibular schwannomas by its position eccentric to the IAC and frequent broad dural contact with a presence of a dural tail (Fig. 12). Though, in practice, it can sometimes be difficult to differentiate meningiomas and schwannomas. Meningiomas occur in the adult population.

Lipomas in the IAC demonstrate their typical appearance, with loss of the T1 hyperintensity on fat-suppressed sequences. Lipomas are often times found incidentally in patients of

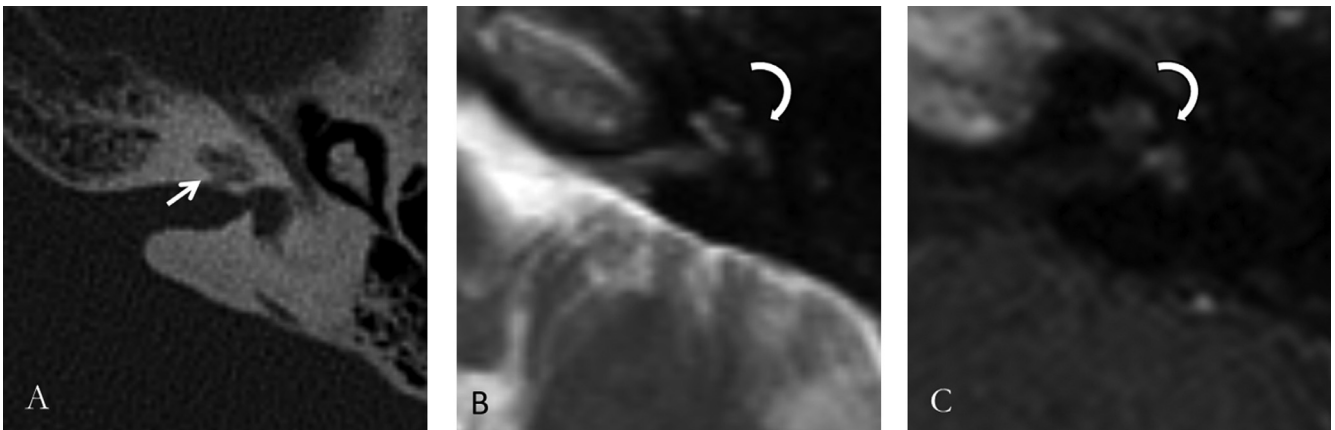


**Figure 8** CT image (A) demonstrates near-total ossification of the cochlea (arrow). T2-weighted imaging (B) shows loss of the normal T2 hyperintense signal within the cochlea, vestibule, and semicircular canals (curved arrow). Postcontrast T1 weighted imaging (C) shows patchy enhancement in the same inner ear structures (curved arrow).

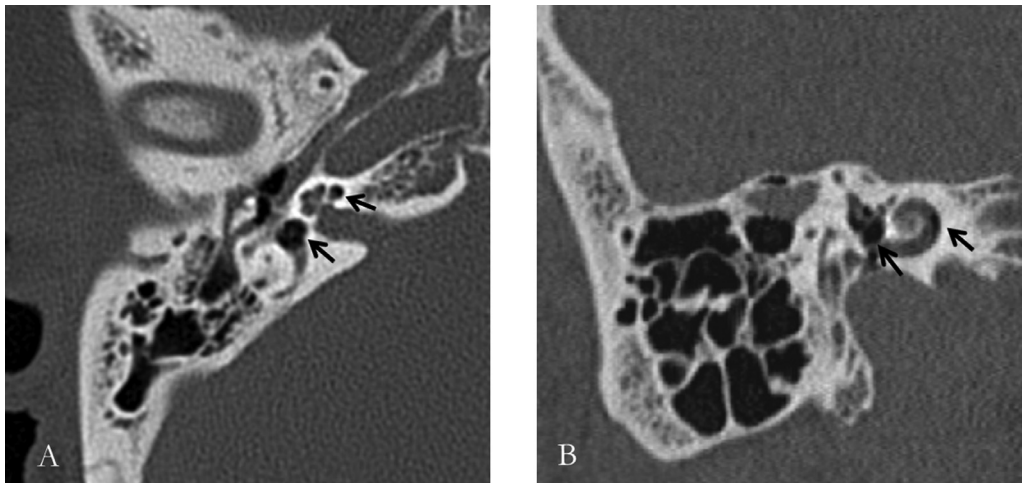


**Figure 9** Axial and coronal CT section of the temporal bones (A, B) demonstrating multiple foci of pneumolabyrinth within the cochlea and vestibule (arrows).

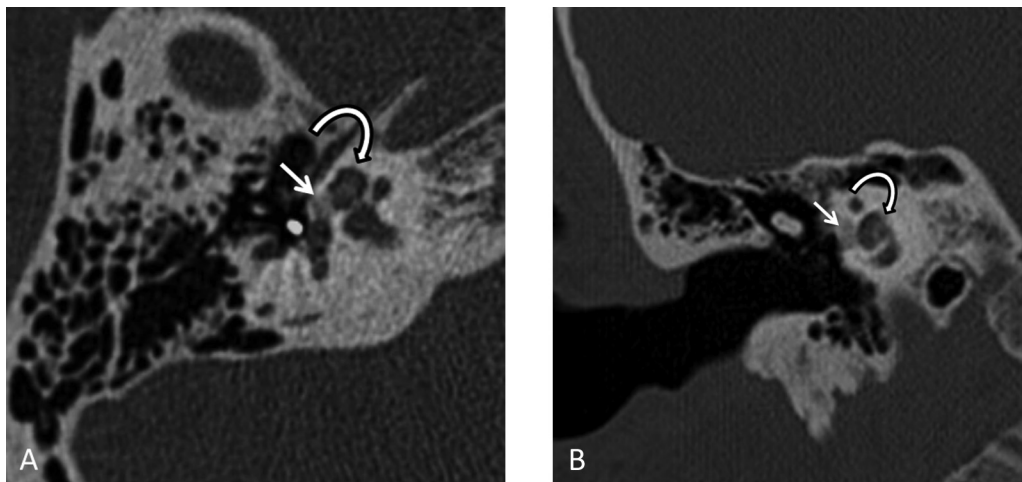


**Figure 10** Axial and coronal CT section of the right temporal bone (A, B) demonstrating focal demineralization (arrow) of the otic capsule lateral to the cochlea (curved arrow) and anterior to the oval window consistent with fenestral otosclerosis

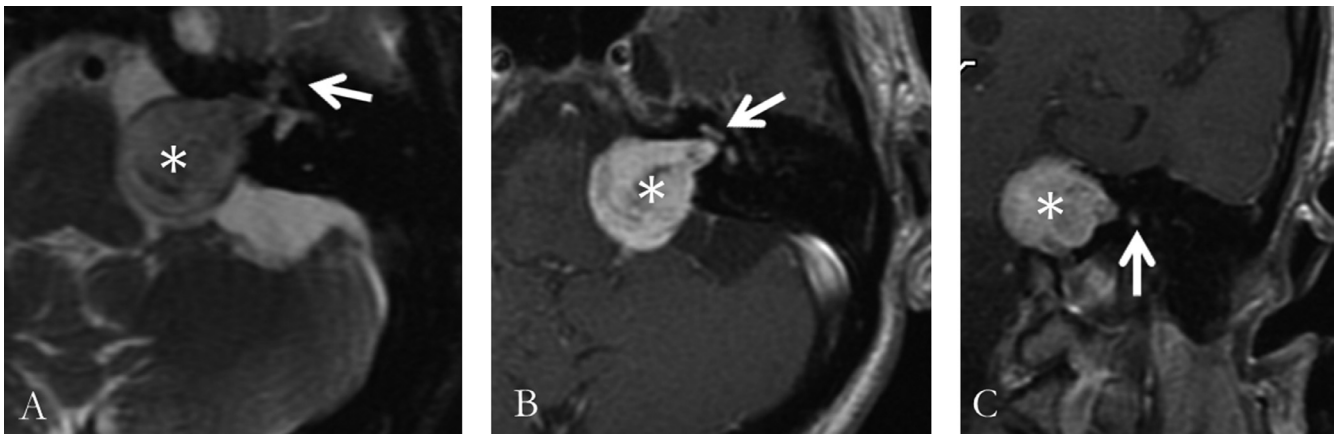


**Figure 11** Axial T2-weighted image (A) shows a large T2 hyperintense cerebellopontine angle mass (asterisk) that expands and widens the IAC, with loss of the normal T2 signal within the cochlea (arrow). Axial and coronal post-contrast T1-weighted images (B and C) show avid enhancement of the mass (asterisk) with an “ice cream cone” appearance (large scoop). There is abnormal enhancement extending into the cochlea (arrow) consistent with intralabyrinthine involvement.

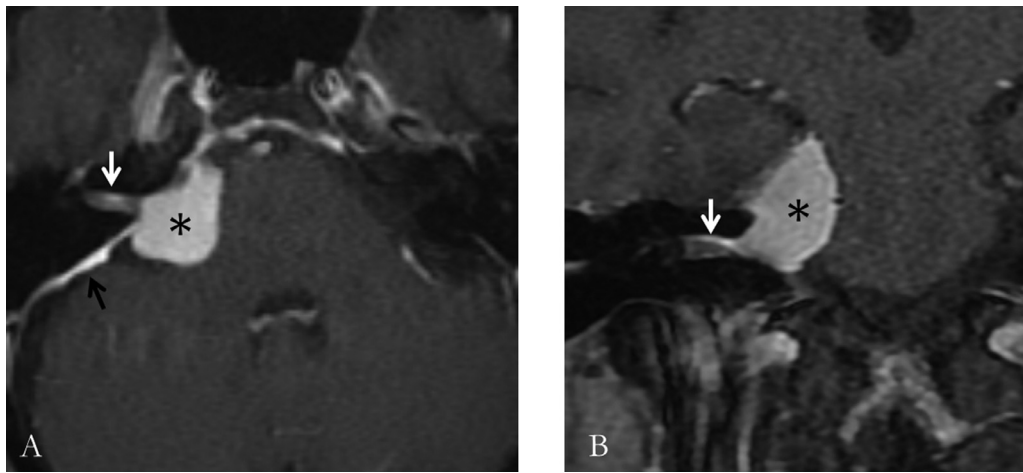


**Figure 12** Axial and coronal T1-weighted post-contrast images of the right IAC (A, B) show an enhancing CPA mass (asterisk) with a broad dural attachment (black arrow). There is slight extension of the enhancement into the IAC (white arrow), but the mass is predominantly centered outside the IAC.

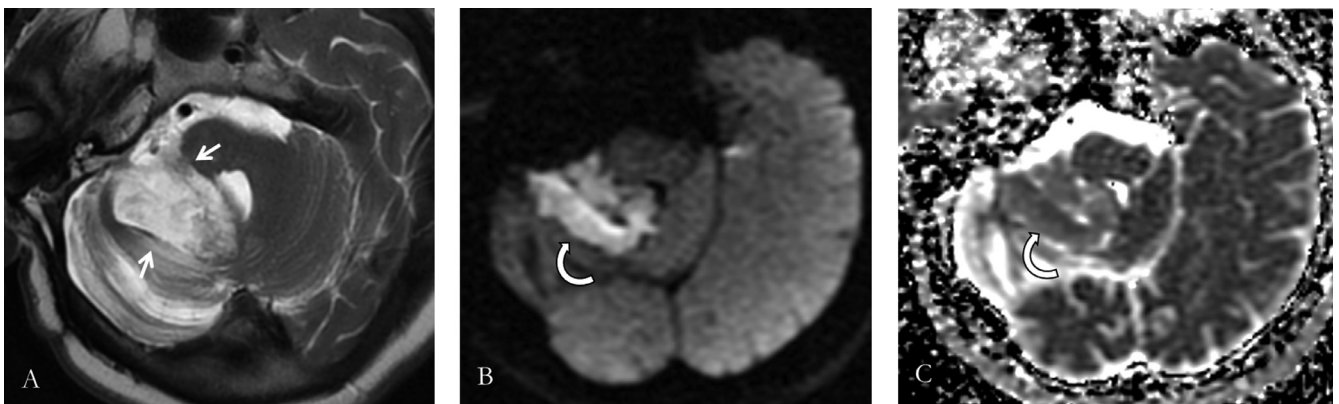


**Figure 13** Axial T2-weighted image (A) shows a T2 hyperintense mass in the region of the right CPA and IAC (arrows). DWI and ADC map axial images (B, C) show restricted diffusion of this lesion (curved arrows), differentiating it as an epidermoid cyst as opposed to an arachnoid cyst.

all ages and are asymptomatic, but rare intravestibular lipomas can result in sensorineural hearing loss.<sup>18</sup>

Epidermoid and arachnoid cysts can have similar appearances, with hyperintense T2 signal and hypointense T1 signal. Depending on the size of the lesion, both epidermoid and arachnoid cysts can have variable signal suppression on FLAIR sequence. However, epidermoids demonstrate diffusion restriction while arachnoid cysts do not (Fig. 13). IAC epidermoids have a mean age of presentation of 27 years, but can occur in patients as young as 8 years.<sup>19</sup> These lesions are frequently asymptomatic but can have mass effect and insinuate between the cisternal and canalicular segments of the IAC cranial nerves.

## Conclusion

There are a wide range of conditions that can cause sensorineural hearing loss, both congenital and acquired. Knowledge of temporal bone anatomy is the first step in determining the etiology. CT and MRI can help with identification of an underlying structural cause. As always, clinical history of the patient's presentation, underlying conditions, and physical exam and audiology findings are helpful in enabling the radiologist to make the correct diagnosis. Awareness of disease processes specific to the patient's age of presentation will help narrow the possibilities.

## References

1. Shekdar KV, Bilaniuk LT: Imaging of pediatric hearing loss. *Neuroimaging Clin N Am* 29:103-115, 2019. <https://doi.org/10.1016/j.nic.2018.09.011>
2. Nash SD, Cruickshanks KJ, Klein R, et al: The prevalence of hearing impairment and associated risk factors: The beaver dam offspring study. *Arch Otolaryngol - Head Neck Surg* 137:432-439, 2011. <https://doi.org/10.1001/archoto.2011.15>
3. Weissman JL: Hearing loss. *Radiology* 199:593-611, 1996. <https://doi.org/10.1148/radiology.199.3.8637972>
4. Vijayasekaran S, Halsted MJ, Boston M, et al: When is the vestibular aqueduct enlarged? A statistical analysis of the normative distribution of vestibular aqueduct size. *Am J Neuroradiol*. 28:1133-1138, 2007. <https://doi.org/10.3174/ajnr.A0495>
5. Pont E, Mazón M, Montesinos P, et al: Imaging diagnostics: Congenital malformations and acquired lesions of the inner ear. *Acta Otorrinolaringol Esp* 66:224-233, 2015. <https://doi.org/10.1016/j.otorri.2014.07.002>
6. Lowe LH, Vézina LG: Sensorineural hearing loss in children. *RadioGraphics* 17:1079-1093, 1997. <https://doi.org/10.1148/radiographics.17.5.9308102>
7. Ozgen B, Oguz KK, Atas A, et al: Complete labyrinthine aplasia: Clinical and radiologic findings with review of the literature. *Am J Neuroradiol* 30:774-780, 2009. <https://doi.org/10.3174/ajnr.A1426>
8. Huang BY, Zdanski C, Castillo M: Pediatric sensorineural hearing loss, part 1: Practical aspects for neuroradiologists. *Am J Neuroradiol* 33:211-217, 2012. <https://doi.org/10.3174/ajnr.A2498>
9. Joshi VM, Shantanu Navlekar BK, Ravi Kishore BG, et al: CT and MR imaging of the inner ear and brain in children with congenital sensorineural hearing loss. *Radiographics* 32:683-698, 2012. <https://doi.org/10.1148/rg.323115073>
10. Sennaroglu L, Bajin MD: Classification and current management of inner ear malformations. *Balkan Med J* 34:397-411, 2017. <https://doi.org/10.4274/balkanmedj.2017.0367>
11. Sennaroglu L, Saatci I: A new classification for cochleovestibular malformations. *Laryngoscope* 112:2230-2241, 2002. <https://doi.org/10.1097/00005537-200212000-00019>
12. Prabhu SP, Prabhu SP, Huang L, et al: Frequent association of cochlear nerve canal stenosis with pediatric sensorineural hearing loss. *Arch Otolaryngol Neck Surg* 138:383, 2012. <https://doi.org/10.1001/archoto.2012.237>
13. Little SC, Kesser BW: Radiographic classification of temporal bone fractures: Clinical predictability using a new system. *Arch Otolaryngol - Head Neck Surg* 132:1300-1304, 2006. <https://doi.org/10.1001/archotol.132.12.1300>
14. Mun SK, Oh KH, Hong YH, et al: Using temporal bone computed tomography to predict sensorineural hearing loss in otic capsule-sparing temporal bone fracture. *Injury* 48:2879-2883, 2017. <https://doi.org/10.1016/j.injury.2017.10.041>
15. Andreu-Arasa VC, Sung EK, Fujita A, et al: Otosclerosis and dysplasias of the temporal bone. *Neuroimaging Clin N Am* 29:29-47, 2019. <https://doi.org/10.1016/j.nic.2018.09.004>
16. Lin EP, Crane BT: The management and imaging of vestibular schwannomas. *Am J Neuroradiol* 38:2034-2043, 2017. <https://doi.org/10.3174/ajnr.A5213>
17. Skolnik AD, Loevner LA, Sampathu DM, et al: Cranial nerve Schwannomas: Diagnostic imaging approach. *RadioGraphics* 36:1463-1477, 2016. <https://doi.org/10.1148/rg.2016150199>
18. Dahlen RT, Johnson CE, Harnsberger HR, et al: CT and MR imaging characteristics of intravestibular lipoma. *Am J Neuroradiol* 23:1413-1417, 2002. <http://www.ncbi.nlm.nih.gov/pubmed/12223388>
19. deSouza CE, DeSouza R, da Costa S, et al: Cerebellopontine angle epidermoid cysts: A report on 30 cases. *J Neurol Neurosurg Psychiatry* 52:986-990, 1989. <http://www.ncbi.nlm.nih.gov/pubmed/2795068>